Biomechanical assessment predicts aneurysm-related events in patients with abdominal aortic aneurysm

Biomechanical assessment predicts aneurysm-related events in patients with abdominal aortic aneurysm

Barry J. Doyle,[a,b,c,d] Nikhilesh Bappoo,[a,b] Maaz Syed,[c] Rachael O. Forsythe,[c] Janet T. Powell,[e] Noel Conlisk,[c] Peter R. Hoskins,[c] Grand Roman Joldes,[b] Olivia M.B. McBride,[c] Anoop S.V. Shah,[c] Paul E. Norman,[a,f] David E. Newby[c]

a. Vascular Engineering Laboratory, Harry Perkins Institute of Medical Research, QEII Medical Centre, Nedlands and Centre for Medical Research, The University of Western Australia, Perth, Australia.
b. School of Engineering, The University of Western Australia, Perth, Australia.
c. BHF Centre for Cardiovascular Science, The University of Edinburgh, Edinburgh, UK.
d. Australian Research Council Centre for Personalised Therapeutics Technologies, Australia
e. Vascular Surgery Research Group, Imperial College London, London, UK.
f. Medical School, The University of Western Australia, Perth, Australia.

Running head: Biomechanical assessment of aortic aneurysm

Address for Correspondence:

Name:	Barry Doyle
Address:	Harry Perkins Institute of Medical Research, 6 Verdun Street, Nedlands, Western Australia, 6009, Australia.
Tel:	+61 8 6151 1084
Fax:	+61 8 6151 1084
Email:	barry.doyle@uwa.edu.au
Twitter:	@vasclab_uwa

What does this study add?

This is the first prospective study to test if a biomechanical assessment of abdominal aortic aneurysm at baseline predicts future events. We show that the aneurysm biomechanical ratio of wall stress to wall strength is independently associated with future aneurysm rupture and repair, after incorporating known risk factors such as diameter. The methods used are robust and determining the aneurysm biomechanical ratio could be a useful adjunct to diameter and help guide the management of patients with abdominal aortic aneurysm.

Abstract

Objectives Improved methods of rupture prediction is a priority in abdominal aortic aneurysm (AAA). Biomechanical analysis of risk in AAA has major clinical potential but lacks robust evidence that it adds clinical value. We aimed to test if the aneurysm biomechanical ratio (ABR, a dimensionless ratio of wall stress and wall strength) can predict aneurysm-related events.

Methods In a prospective multicentre clinical study of 295 patients with AAA (diameter ≥ 40 mm), we used three-dimensional reconstruction and computational biomechanical analyses to compute ABR at baseline. Participants were followed for at least two years and the primary endpoint was the composite of aneurysm rupture or repair.

Results The majority were male (87%) current or former smokers (86%), most (72%) had hypertension (mean systolic blood pressure of 140±22 mmHg) and mean baseline diameter was 49.0±6.9 mm. Mean ABR was 0.49±0.27. Rupture (n=13) or repair (n=102) occurred in 115 (41%) cases. The number of repairs increased across tertiles of ABR; low (n=24), medium (n=34), high ABR (n=44) (p=0.010). Rupture or repair occurred more frequently in those with higher ABR (log rank p=0.009) and ABR was independently predictive of this outcome after adjusting for diameter and other clinical risk factors, including gender and smoking (hazard ratio, 1.41; 95% confidence interval, 1.09-1.83; p=0.010).

Conclusions We have shown that the biomechanical ABR is a strong independent predictor of AAA rupture or repair in a model incorporating known risk factors, including diameter. Determining ABR at baseline could help guide the management of patients with AAA.

Keywords (MeSH): Abdominal aortic aneurysm; peripheral vascular disease; computational biomechanics; imaging.

Introduction

Abdominal aortic aneurysm (AAA) rupture is associated with up to 90% mortality and only 50-70% of those who reach hospital survive.[1] Given the typically asymptomatic nature of AAAs, most are found incidentally or through screening studies.[2] When detected, pre-emptive surgical repair is usually offered when the maximum anterior-posterior aneurysm diameter reaches 50-55 mm. However, despite the strong association between diameter and risk of rupture,[3-5] there remain cases that rupture at smaller diameters[6] (especially in women[7]) and cases that grow large despite never rupturing.[8] In fact, for those with aneurysm greater than 55 mm the risk of death from causes other than AAA is higher than the risk of death from rupture.[9] This uncertainty has stimulated interest in alternative methods to identify cases that are more likely to rupture, and hence benefit from surgical intervention.

One approach is the biomechanical assessment of AAA stability using calculations of wall stress with the finite element method. Computational methods have now progressed to the point of semi-automated analyses.[10,11] Many reports describe the possible clinical benefit of peak wall stress (PWS)[12-16] and the use of a dimensionless ratio of wall stress and wall strength.[10,17,18] Yet, despite such metrics being noted in clinical guidelines as factors that influence rupture,[19] there is a clear lack of evidence to support their use.[20] Data thus far have been limited by factors ranging from small sample sizes to the non-standardised and arbitrary methods used to calculate wall stress. Consequently, a systematic review of the literature established that none of the proposed biomechanical imaging markers are conclusively associated with growth or rupture.[21]

We reported a new method[22] to compute wall stress in AAAs that overcomes the obstacles of requiring unattainable patient-specific material properties while also incorporating

measurements of wall thickness.[11] Our hypothesis is that this new approach will provide more patient-specific calculations of risk and be a better predictor of clinical outcome than diameter. To test this, we applied our technique in a prospective study to determine if patient-specific aneurysm biomechanical ratio (ABR, i.e. the dimensionless ratio of wall stress and wall strength) at baseline predicts the combined outcome of aneurysm rupture and/or repair.

Methods

This study is reported in line with the STROBE statement[23] and a detailed description of the Methods, along with the STROBE checklist (Table S1) are available in the Supplementary Material.

Study design, setting and population

This was a multicentre cohort study performed as part of the MA^{3}RS Study (ISRCTN76413758).[24,25] All patients gave informed consent and were selected based on AAA diameter ≥ 40 mm measured by ultrasound and under ultrasound surveillance as part of routine care. A full description of inclusion/exclusion criteria is provided in the Supplementary Material.

Study protocol and follow-up

Within six weeks of the initial screening ultrasound, participants underwent full clinical assessment, including blood pressure measurement, MRI and computed tomography angiography (CTA). Patients were then reviewed every six months for a minimum of 24 months. The full protocol is available elsewhere.[25] Briefly, patients were imaged using a 3T Siemens Magnetom Verio scanner using a respiratory-gated, T2-weighted (T2W) turbo spin echo sequence (TR/TE 2500/252 ms; matrix 365×384; field of view 300×400 mm; slice

width 5 mm) acquired with and without Spectral Attenuated Inversion Recovery fat suppression in order to allow segmentation of aortic wall. CTA was performed using a 320-multidetector (Edinburgh: Aquilon ONE; Toshiba) or 64-multidetector CT scanner (Glasgow: Brilliance 64; Philips).

Biomechanical analyses at baseline

The methods used are described in detail elsewhere[11] and also in the Supplementary Material. Briefly, after 3D reconstruction of the MRI and CTA data, the computational biomechanics processes are fully automated and output the required data.[11] Patient-specific baseline blood pressure is applied to the inner surface of the lumen and the AAA geometry is fixed from movement in all directions in the proximal and distal regions to represent attachment to the proximal non-aneurysmal aorta and distally to the iliac arteries (Figure S1).[10-18] The 3D reconstruction method can introduce user variability, however we[11] and others[26] have demonstrated that resulting biomechanical data are relatively insensitive to variations in 3D reconstruction. Our algorithm calculates maximum principal wall stress, wall strength[27] and ABR.[17] ABR is the ratio of local wall stress to local wall strength and we use the 99th centile of ABR as the final patient-specific metric, which we refer to as peak ABR throughout this study. We also investigated the spatial locations of peak ABR in each case (Figure S3).

Statistical analysis

The sample size was calculated for the original MA^{3}RS Study.[25] The primary endpoint was the composite of two aneurysm-related events, AAA repair and/or rupture. Biomechanical and statistical analyses were performed independently to minimize bias, with the primary biomechanical analysts (BJD, NB) blinded to the clinical endpoint data and all statistical analyses performed by independent analysts (MS, ASVS). As with the original MA^{3}RS

Study, treating clinicians were blind to all research imaging and image processing data and their decision to intervene was unbiased by the study. Categorical data are presented as counts and percentage, whereas continuous data are presented as mean ± standard deviation (SD). Correlations were determined using two-sided Pearson's or Spearman's tests. Peak ABR and PWS were logarithmically transformed and we stratified our cohort by tertiles of peak ABR. We used ANOVA to determine differences in baseline risk factors and Kaplan-Meier analysis to evaluate the time to event for each group. To assess the power of ABR to predict the primary endpoint, a Cox regression model was developed with variables iteratively included to the model.

We developed three models:

- *Model 1* = unadjusted;
- *Model 2* = Model 1 plus age (y), sex and baseline diameter measured with ultrasound (mm);
- *Model 3* = Model 2 plus smoking status, systolic and diastolic blood pressure (mmHg), diabetes and uptake of USPIO.

Aneurysm growth rate was determined from serial ultrasound measurements using a linear regression model fit to all available ultrasound data, with the slope used to determine growth rate per year. Aneurysm growth rate was then investigated as a post hoc outcome. Finally, we also investigated the categorical net reclassification index (NRI_{cat}) using two different risk thresholds (0.5 and 0.8), then the continuous NRI (NRI_{cont}) and finally the integrated discrimination index (IDI). The NRI quantifies how well a new model reclassifies subjects, either appropriately or inappropriately, as compared to an old model. Whereas, the IDI quantifies the capacity of a marker to predict a binary outcome of interest. Statistical significance was deemed at two-sided $p<0.05$.

RESULTS

Baseline characteristics of the cohort are shown in Table 1. Of the 1942 patients originally screened, 295 were included in the study (Figure 1), with more detail provided in the Supplementary Material. We excluded 14% (47/342) of the original MA^{3}RS cohort due to absent or inadequate CTA, however our final cohort had similar baseline characteristics to the original cohort (see Supplementary Material, Table S2).

Baseline biomechanical assessment

We divided the cohort into tertiles of peak ABR as follows: Tertile 1 = 0.16-0.36; Tertile 2 = 0.37-0.49; Tertile 3 = 0.50-2.32. Baseline diameter was different across the tertiles of peak ABR ($p=0.008$), being lowest in the lowest ABR tertile (Table 1). The proportion of women increased across the ABR tertiles ($p<0.001$). All biomechanical data are shown in Table 2 with an illustrative case shown in Figure 2. There were a number of significantly different biomechanical variables across ABR tertiles (Table 2).

Increasing baseline diameter was correlated weakly with both peak ABR ($r=0.158$, $p=0.006$) and PWS ($r=0.135$, $p=0.019$). ABR and PWS were correlated with both wall thickness ($r=0.274$, $p<0.001$ and $r=0.278$, $p<0.001$, respectively) and ILT thickness ($r=0.194$, $p<0.001$ and $r=0.345$, $p<0.001$, respectively). Furthermore, ABR and PWS were both correlated with AAA wall strength ($r=-0.274$, $p<0.001$ and $r=0.202$, $p<0.001$, respectively; Figure S2). The location of peak ABR was variable throughout the cohort, however, there was a clear tendency to occur on the left side (49%) compared to the right (23%), posterior (16%), or anterior (12%). Also, the left medial region was the most common location (15%), followed by the posterior medial (9%), anterior medial (7%) and posterior left medial regions (7%; Table S3 and S4). However peak ABR also occurred outside the zone of maximum diameter

(medial region) in a about half the cases, more proximal in 30% and more distal in 22%. Interestingly, heat maps of location and peak ABR show that the right medial region experience the greatest magnitude of ABR (Figure S4).

Clinical follow-up and the primary endpoint

Participants were followed up for a mean of 848±379 days. The mean growth rate of the cohort was 2.84±2.54 mm/year (n=249; see Supplementary Material) and was similar across ABR tertiles (p=0.349; Table 1).

Rupture (n=13) or repair (n=102) occurred in 115 (41%) cases; 98 repairs were elective, of which 40 were endovascular aneurysm repair and the remainder were open repair. Cases with an aneurysm-related event more commonly had peak ABR on the left side (52%) over the right (21%), posterior (15%), or anterior sides (12%). Again, the left medial region was the dominant location of peak ABR (17%) in cases with an aneurysm-related event; 31% of ruptures (4/13) occurred on the left medial wall (Table S3).

The mean (standard error) log-transformed peak ABR of cases that had a clinical event was 16% higher than those without (-0.86 (0.03) vs. -0.74 (0.04); p=0.0138; Figure 3A). The number of repairs increased from low (n=24) to medium (n=34) and high (n=44) ABR tertiles (p=0.010), however the number of ruptures did not (p=0.3575; Table 3). In total, there were 39 (13%) deaths of which 31% (12/39) were AAA-related (11 from AAA rupture and one from gut ischaemia after repair) and 28% (11/39) were from other cardiovascular-related causes.

Duration of follow-up was similar for each tertile (p=0.346). As shown in the Kaplan Meier analysis (Figure 3B), repair or rupture occurred more frequently in those with higher peak ABR (log rank p=0.0089). Cox regression (Table 4) revealed peak ABR tertiles to be independently predictive of the primary endpoint after adjusting for age, sex, baseline diameter, smoking status, systolic and diastolic blood pressure, diabetes, and inflammation of the AAA wall. In a post hoc analysis of AAA growth rate and using an annual growth rate of 2.5 mm/y as a threshold for above average growth,[28] we found that for unadjusted data, ABR was associated with AAA growth rate (Model 1 = HR 1.51, 95% CI 1.29-1.77, p<0.001) but this association lost significance after adjustment for confounding factors (including baseline diameter, smoking and diabetes) (Model 2 = HR 1.58, 95% CI 0.73-3.41, p=0.248; Model 3 = HR 1.32, 95% CI 0.49-3.53, p=0.586) (Figures S5-7).

At a risk threshold of 0.5 the NRI_{cat} value was 0.011 (95% CI, -0.064-0.086; p=0.769) with 8 cases reclassified up to a higher risk and 23 reclassified down to a lower risk, whereas at a threshold of 0.8, the NRI_{cat} value was 0.066 (95% CI, -0.011-0.142; p=0.093) with 16 cases reclassified up and 7 reclassified down. These NRI_{cat} data suggests that 1.1% and 6.6% of cases with outcome are more likely to move up a risk category rather than down, respectively (see Supplementary Material, Figures S8-11). The NRI_{cont}, which assesses whether change in predicted risk is in the correct direction, was 0.327 (95% CI, 0.095-0.560; p=0.006) and the IDI was 0.023 (95% CI, 0.005-0.042; p=0.015).

DISCUSSION

Estimating the likelihood of abdominal aortic aneurysm rupture has major potential clinical benefit. Over recent decades, computational biomechanics methods have been the focus of much research, although there remains no strong evidence that such risk assessment methods

provide any benefit to the patient. Here we report the first and largest prospective clinical study to test if the aneurysm biomechanical ratio (ABR) can help stratify patients. We show that the peak ABR computed at baseline is a major predictor of repair or rupture, independent of all risk factors, including age, sex, aneurysm diameter and smoking. Our findings suggest that biomechanical risk profiling at baseline using combined CTA and MRI could help inform clinical decisions about the timing of elective repair.

There has been much recent effort in contemporary 3D tools and image-based AAA assessment methods.[10,11,29,30] Importantly for clinicians, current image-based biomechanical approaches to AAA rupture risk are straightforward to implement and do not require significant specialist training. In fact, within hours an individual with knowledge of AAA and basic computing skills can be trained in such frameworks, and as all data besides the 3D reconstruction are automatic and thus insensitive to user-variation, biomechanical data are repeatable.[11] Once trained, the 3D reconstruction process takes < 1 hour and as with most tasks, this reduces with familiarity, so that even a novice user with no previous AAA 3D reconstruction experience can reproduce ABR to within 5% of expert results.[11] Therefore, expertise in computational biomechanics is not a barrier to translation.

Here we have shown that patients with high peak ABR at baseline were more likely to have an aneurysm-related event in a cohort of patients with extended follow up, where the treating clinician was unaware of the biomechanical findings and where ABR was adjusted for clinical risk factors including AAA diameter. This blinding and adjustment is a major strength as AAA diameter and sex currently inform the timing of elective repair: peak ABR was independently predictive of the primary outcome. Therefore, we also evaluated how peak ABR might alter the classification of patients who should be offered elective AAA repair. For

thresholds of 0.5 and 0.8 peak ABR, the categorical NRI was 1.1% (p=0.796) and 6.6% (p=0.093), respectively, but the continuous NRI was higher and significant at 32.7% (p=0.006). Reclassification measures that are independent of the choice of cut-off, such as the continuous NRI, are perhaps more appropriate as they are not sensitive to arbitrary risk thresholds, however categorical NRI are often easier to interpret. The integrated discrimination index (IDI) was modest, showing a 2.3% increase through the addition of peak ABR, however the finding was significant (p=0.015) and similar IDI increases of 2-3% have been reported in other cardiovascular studies that assessed the value of new risk markers in larger cohort sizes.[31]

In contrast to our promising data, a recent retrospective study[32] of 175 intact, 11 symptomatic and 45 ruptured AAAs, reported no added value of biomechanical indices in risk assessment using commercially available software (A4research™). They used ROC-analysis to determine that various combinations of biomechanical data did not offer improvement over diameter alone. However, unlike our methods, they relied on assumptions of AAA wall thickness and material properties for both the AAA wall and ILT.

Wall thickness has a strong influence on wall stress and subsequent biomechanical metrics. We measured large inter- and intra-variation in wall thickness in our cohort, and previous work has shown the influence of wall thickness on PWS.[33] Therefore, variation in AAA wall thickness exists and should be included into biomechanical models (see Supplementary Material, Tables S5-7). However, the requirement for wall thickness presents initial problems if trying to implement the ABR into the clinic as MRI is not routine in AAA management and using CTA alone for wall thickness measurement is not straightforward, except in the uncommon situation when intraluminal thrombus is absent.[33] The MA^{3}RS Study showed that

the uptake of USPIO on MRI predicts growth and clinical outcome.[24] As such, MRI could serve (at least) two roles in contemporary AAA care; quantify inflammation via USPIO and provide wall thickness data.

Our study has several further strengths. To the best of our knowledge, this is the first prospective study of AAA biomechanical methods and has used a well-planned clinical trial with a high predicted[34] and actual event rate (41%)[24] which was 39% in this current study. This study was designed to evaluate the role of peak ABR in aneurysm-related events. It is clear from our study that those with high baseline ABR are more likely to have a future aneurysm-related event (Figure 3B). We also observed the anatomical location of peak ABR across the AAA to be variable, as is the area of peak ABR. However, we noted a clear propensity for peak ABR to occur on the left lateral wall (49%), or more specifically, the left lateral medial wall, in both intact (14%) and cases that ruptured (31%) or needed repair (13%). In the seminal work of Darling et al.[8] they report that 74% of cases ruptured into the retroperitoneum, with 33% on the left posterior-lateral and 26% on the right posterior-lateral side. In our previous work,[15] we also observed the location of rupture to be the left posterior-lateral region, with this location predicted by our biomechanical simulation using imaging acquired four months before rupture. Given the potential utility of ABR demonstrated in this study, future studies will evaluate whether additional information about the anatomical location, gradient of ABR or extent of raised ABR would increase the discrimination of future AAA clinical events. These can be studied from our existing database but would benefit from validation in a separate cohort.

There are some limitations of our work. First, despite being the largest study of its kind and although we examined 295 patients, due to unforeseen logistical obstacles we lost 47 cases

due to missing CTA (n=31) and some due to poor quality CTA (n=16). The study was underpowered to assess the impact of ABR on aneurysm rupture alone, but is powered for the composite of rupture and/or repair. Second, as discussed earlier, MRI is not routine in AAA and as such, our methods would incur an additional cost to implement clinically. However, the cost of a single MRI is considerably less than the cost of (unnecessary) intervention.[35] Third, we did not include the aortic wall calcifications in our study as they introduce further uncertainty. Li et al[36] included calcifications and found that they increased wall stress by 14% (range 2-27%, $p<0.01$). However, others have reported the opposite, with reductions in wall stress from 10-59%.[37] Fourth, the estimation of wall strength[27] depends in part on the family history of AAA, which may not be precise since it is subject to recall and other biases, such as premature mortality. Fifth, there was no precise protocol for the timing of elective repair, which was left to clinical discretion, although the treating clinician had no knowledge of either USPIO uptake or ABR: the study data collection did not include the exact reason(s) prompting the timing of elective repair. Finally, our methods would benefit from external validation in an independent dataset before recommendations can be made to modify guidelines.

CONCLUSIONS

We have shown for the first time that the aneurysm biomechanical ratio independently predicted the combined outcome of abdominal aortic aneurysm repair or rupture. Furthermore, the aneurysm biomechanical ratio may prove to be a better predictor of aneurysm-related events than maximum diameter. Our data are encouraging and a larger prospective trial should be undertaken to verify our findings and determine if such methods could be introduced as an adjunct assessment in routine patient management.

ACKNOWLEDGEMENTS

We would like to thank Arjun Balaji (UWA) for his assistance with aneurysm reconstructions.

SOURCES OF FUNDING

This work was funded by the National Health and Medical Research Council (NHMRC) (APP1063986). The MA^{3}RS Study was funded by Medical Research Council (MRC) and managed by National Institute of Healthcare Research (NIHR) on behalf of the MRC-NIHR partnership (NIHR Efficacy and Mechanism Evaluation Programme: funding reference 11/20/03). BJD acknowledges support from the NHMRC Career Development Award (APP1083572). GRJ acknowledges support from a Merit Award from the Department of Health, Western Australia. DEN is supported by the British Heart Foundation (CH/09/002) and is the recipient of a Wellcome Trust Senior Investigator Award (WT103782AIA). The Edinburgh Clinical Research Facility and Clinical Research Imaging Centre are supported by NHS Research Scotland.

DISCLOSURES

The authors have no disclosures to make.

REFERENCES

1. Kent KC. Clinical practice. Abdominal aortic aneurysms. *N Engl J Med*. 2014;371:2101-8.
2. Wanhainen A, Hultgren R, Linne A, Holst J, Gottsater A, Langenskiold M, et al. Outcome of the Swedish Nationwide Abdominal Aortic Aneurysm Screening Program. *Circulation*. 2016;134:1141-1148.

3. Powell JT, Brown LC, Forbes JF, Fowkes FG, Greenhalgh RM, Ruckley CV and Thompson SG. Final 12-year follow-up of surgery versus surveillance in the UK Small Aneurysm Trial. *Br J Surg*. 2007;94:702-8.

4. Lederle FA, Johnson GR, Wilson SE, Ballard DJ, Jordan WD, Jr., Blebea J, et al. Rupture rate of large abdominal aortic aneurysms in patients refusing or unfit for elective repair. *JAMA*. 2002;287:2968-72.

5. Lederle FA, Johnson GR, Wilson SE, Chute EP, Hye RJ, Makaroun MS, et al. The aneurysm detection and management study screening program: validation cohort and final results. Aneurysm Detection and Management Veterans Affairs Cooperative Study Investigators. *Arch Intern Med*. 2000;160:1425-30.

6. Powell JT, Gotensparre SM, Sweeting MJ, Brown LC, Fowkes FGR and Thompson SG. Rupture Rates of Small Abdominal Aortic Aneurysms: A Systematic Review of the Literature. *Eur J Vasc Endovasc Surg*. 2011;41:2-10.

7. Lo RC, Lu B, Fokkema MT, Conrad M, Patel VI, Fillinger M, Matyal R and Schermerhorn ML. Relative importance of aneurysm diameter and body size for predicting abdominal aortic aneurysm rupture in men and women. *J Vasc Surg*. 2014;59:1209-16.

8. Darling R, Messina C, Brewster D and Ottinger L. Autopsy study of unoperated abdominal aortic aneurysms. The case for early resection. *Circulation*. 1977;56:II161 - II164.

9. Parkinson F, Ferguson S, Lewis P, Williams IM and Twine CP. Rupture rates of untreated large abdominal aortic aneurysms in patients unfit for elective repair. *J Vasc Surg*. 2015;61:1606-1612.

10. Gasser TC, Auer M, Labruto F, Swedenborg J and Roy J. Biomechanical rupture risk assessment of abdominal aortic aneurysms: model complexity versus predictability of finite element simulations. *Eur J Vasc Endovasc Surg*. 2010;40:176-85.

11. Joldes GR, Miller K, Wittek A, Forsythe RO, Newby DE and Doyle BJ. BioPARR: A software system for estimating the aneurysm biomechanical ratio for abdominal aortic aneurysms. *Sci Rep*. 2017;7:4641.

12. Fillinger M, Marra S, Raghavan M and Kennedy F. Prediction of rupture risk in abdominal aortic aneurysm during observation: wall stress versus diameter. *J Vasc Surg*. 2003;37:724 - 732.

13. Fillinger M, Raghavan M, Marra S, Cronenwett J and Kennedy F. In vivo analysis of mechanical wall stress and abdominal aortic aneurysm rupture risk. *J Vasc Surg*. 2002;36:589 - 597.

14. Doyle BJ, Callanan A, Burke PE, Grace PA, Walsh MT, Vorp DA and McGloughlin TM. Vessel asymmetry as an additional diagnostic tool in the assessment of abdominal aortic aneurysms. *J Vasc Surg*. 2009;49:443-454.

15. Doyle BJ, McGloughlin TM, Miller K, Powell JT and Norman PE. Regions of high wall stress can predict the future location of rupture of abdominal aortic aneurysm. *Cardiovasc Intervent Radiol*. 2014;37:815-8.

16. Venkatasubramaniam A, Fagan M, Mehta T, Mylankal K, Ray B, Kuhan G, et al. A comparative study of aortic wall stress using finite element analysis for ruptured and non-ruptured abdominal aortic aneurysms. *Eur J Vasc Endovasc Surg*. 2004;28:168 - 176.

17. Vande Geest JP, Di Martino ES, Bohra A, Makaroun MS and Vorp DA. A biomechanics-based aneurysm biomechanical ratio for abdominal aortic aneurysm risk assessment: demonstrative application. *Ann N Y Acad Sci*. 2006;1085:11-21.

18. Maier A, Gee MW, Reeps C, Pongratz J, Eckstein HH and Wall WA. A comparison of diameter, wall stress, and aneurysm biomechanical ratio for abdominal aortic aneurysm rupture risk prediction. *Ann Biomed Eng*. 2010;38:3124-34.

19. Chaikof EL, Brewster DC, Dalman RL, Makaroun MS, Illig KA, Sicard GA, et al. The care of patients with an abdominal aortic aneurysm: the Society for Vascular Surgery practice guidelines. *J Vasc Surg*. 2009;50:S2-49.

20. Wanhainen A, Verzini F, Van Herzeele I, Allaire E, Bown M, Cohnert T, et al. Clinical Practice Guidelines on the Management of Abdominal Aorto-iliac Artery Aneurysms. *Eur J Vasc Endovasc Surg.* 2018;57:8-93.

21. Indrakusuma R, Jalalzadeh H, Planken RN, Marquering HA, Legemate DA, Koelemay MJ and Balm R. Biomechanical Imaging Markers as Predictors of Abdominal Aortic Aneurysm Growth or Rupture: A Systematic Review. *Eur J Vasc Endovasc Surg*. 2016;52:475-486.

22. Joldes GR, Miller K, Wittek A and Doyle B. A simple, effective and clinically applicable method to compute abdominal aortic aneurysm wall stress. *J Mech Behav Biomed Mat*. 2016;58:139-48.

23. von Elm E, Altman DG, Egger M, Pocock SJ, Gøtzsche PC, Vandenbroucke JP. The strengthening of reporting of observational stdies in edpidemiology (STROBE) statement: guidelines for reporting observational studies. *J Clin Epidemiol.* 2008;61:344-99.

24. MA^{3}RS Study Investigators. Aortic Wall Inflammation Predicts Abdominal Aortic Aneurysm Expansion, Rupture, and Need for Surgical Repair. *Circulation*. 2017;136:787-797.

25. McBride OMB, Berry C, Burns P, Chalmers RTA, Doyle B, Forsythe R, et al. MRI using ultrasmall superparamagnetic particles of iron oxide in patients under

surveillance for abdominal aortic aneurysms to predict rupture or surgical repair: MRI for abdominal aortic aneurysms to predict rupture or surgery—the MA^{3}RS Study. *Open Heart*. 2015;2:e000190.

26. Hyhlik-Durr A, Krieger T, Geisbusch P, Kotelis D, Able T and Bockler D. Reproducibility of deriving parameters of AAA rupture risk from patient-specific 3D finite element models. *J Endovasc Ther*. 2011;18:289-98.

27. Vande Geest J, Wang D, Wisniewski S, Makaroun M and Vorp D. Towards a non-invasive method for determination of patient-specific wall strength distribution in abdominal aortic aneurysms. *Ann Biomed Eng*. 2006;34:1098 - 1106.

28. Sweeting MJ, Thompson SG, Brown LC, Powell JT on behalf of the RESCAN Collaborators. Meta-analysis of individual patient data to examine factors affecting growth and rutpure of small abdominal aortic aneurysms. *Br J Surg.* 2012;99:655-65.

29. Gasser TC, Nchimi A, Swedenborg J, Roy J, Sakalihasan N, Bockler D and Hyhlik-Durr A. A novel strategy to translate the biomechanical rupture risk of abdominal aortic aneurysms to their equivalent diameter risk: method and retrospective validation. *Eur J Vasc Endovasc Surg*. 2014;47:288-95.

30. Shum J, Martufi G, Di Martino E, Washington CB, Grisafi J, Muluk SC and Finol EA. Quantitative assessment of abdominal aortic aneurysm geometry. *Ann Biomed Eng*. 2011;39:277-86.

31. Willeit P, Kiechl S, Kronenberg F, Witztum JL, Santer P, Mayr M, et al. Discrimination and Net Reclassification of Cardiovascular Risk With Lipoprotein(a): Prospective 15-Year Outcomes in the Bruneck Study. *JACC*. 2014;64:851-860.

32. Leemans EL, Willems TP, Slump CH, van der Laan MJ and Zeebregts CJ. Additional value of biomechanical indices based on CTa for rupture risk assessment of abdominal aortic aneurysms. *PLOS ONE*. 2018;13:e0202672.

33. Conlisk N, Geers AJ, McBride OM, Newby DE and Hoskins PR. Patient-specific modelling of abdominal aortic aneurysms: The influence of wall thickness on predicted clinical outcomes. *Med Eng Phys*. 2016;38:526-37.

34. Wilson KA, Lee AJ, Hoskins PR, Fowkes FGR, Ruckley CV and Bradbury AW. The relationship between aortic wall distensibility and rupture of infrarenal abdominal aortic aneurysm. *J Vasc Surg*. 2003;37:112-117.

35. Comparative clinical effectiveness and cost effectiveness of endovascular strategy v open repair for ruptured abdominal aortic aneurysm: three year results of the IMPROVE randomised trial. *BMJ*. 2017;359:j4859.

36. Li ZY, J UK-I, Tang TY, Soh E, See TC and Gillard JH. Impact of calcification and intraluminal thrombus on the computed wall stresses of abdominal aortic aneurysm. *J Vasc Surg*. 2008;47:928-35.

37. Maier A, Gee MW, Reeps C, Eckstein HH and Wall WA. Impact of calcifications on patient-specific wall stress analysis of abdominal aortic aneurysms. *Biomech Model Mechanobiol*. 2010;9:511-21.

TABLES

Table 1: Baseline characteristics of the cohort stratified into peak aneurysm biomechanical ratio (ABR) tertiles. Data are mean ± standard deviation unless stated otherwise and p-values are from ANOVA for continuous variables and Chi-squared for categorical variables.

	All cases (n=295)	Tertile 1 **Low ABR** (n=99)	Tertile 2 **Medium ABR** (n=98)	Tertile 3 **High ABR** (n=98)	**p-value**
Characteristics					
Male, n (%)	257 (87.1)	96 (96.9)	86 (87.8)	75 (76.5)	<0.001
Age, y	73.7 ± 7.2	73.4 ± 6.9	73.6 ± 7.8	74.0 ± 6.9	0.837
Smoking status					0.772
Current, n (%)	85 (28.8)	30 (30.3)	33 (33.7)	22 (22.4)	
Previous, n (%)	171 (58.0)	59 (59.6)	53 (54.1)	59 (60.2)	
Never, n (%)	39 (13.2)	10 (10.1)	12 (12.2)	17 (17.3)	
Alcohol, units*	7.5 ± 11.1	7.1 ± 11.7	8.7 ± 11.4	6.7 ± 10.2	0.436
Weight, kg	81.3 ± 14.0	81.9 ± 12.5	80.9 ± 13.8	81.1 ± 15.6	0.855
Height, cm	171.5 ± 8.3	173.1 ± 6.9	171.7 ± 8.4	169.8 ± 9.1	0.021
Systolic blood pressure, mmHg	139.8 ± 24.6	134.2 ± 17.6	137.9 ± 20.0	147.2 ± 24.6	<0.001
Diastolic blood pressure, mmHg	81.4 ± 11.7	79.2 ± 9.2	81.4 ± 10.9	83.7 ± 11.7	0.012
Heart rate, bpm*	70.5 ± 11.4	69.2 ± 9.2	70.2 ± 9.9	72.0 ± 11.4	0.153
Hypertension, n (%)	213 (72.2)	70 (70.7)	72 (73.5)	71 (72.4)	0.909
Aneurysm					
AAA diameter, mm	49.0 ± 6.9	47.3 ± 6.1	50.1 ± 7.7	49.6 ± 6.7	0.008
Growth rate, mm/y	2.84 ± 2.54	2.61 ± 2.49	2.80 ± 2.21	3.17 ± 2.89	0.349
Positive USPIO† uptake, n (%)*	124 (42.6)	43 (43.9)	42 (44.2)	39 (39.8)	0.786
Medical history					
Diabetes, n (%)	42 (14.2)	20 (20.2)	13 (13.3)	9 (9.2)	0.082
Hypercholesterolemia, n (%)	226 (76.6)	78 (78.8)	77 (78.5)	71 (72.4)	0.492
Ischaemic heart disease, n (%)	112 (38.0)	40 (40.4)	46 (46.9)	26 (26.5)	0.011
Peripheral vascular disease, n (%)	58 (19.7)	22 (22.2)	23 (23.5)	13 (13.3)	0.146
Cerebrovascular disease, n (%)	39 (13.2)	18 (18.2)	10 (10.2)	11 (11.2)	0.198
Family history of AAA, n (%)‡	52 (17.6)	4 (4.0)	13 (13.3)	35 (35.7)	<0.001

* Missing data: Growth rate, n=46 (Details provided in the Supplementary Material); alcohol, n=2; heart rate, n=4; USPIO uptake, n=4.

† USPIO = ultrasmall superparamagnetic particles of iron oxide.

‡ Family history of AAA affects wall strength estimation.

Table 2: Baseline biomechanical data of the cohort stratified into peak aneurysm biomechanical ratio (ABR) tertiles. Data are mean ± standard deviation and p-values are from ANOVA.

		Tertile 1	Tertile 2	Tertile 3	
Biomechanical data	**All cases**	**Low ABR**	**Medium ABR**	**High ABR**	**p-value**
Aneurysm biomechanical ratio	0.49 ± 0.27	0.30 ± 0.05	0.43 ± 0.04	0.74 ± 0.34	<0.001
Peak wall stress, MPa	0.35 ± 0.15	0.25 ± 0.04	0.33 ± 0.06	0.48 ± 0.18	<0.001
Wall thickness					
Mean, mm	2.00 ± 0.36	2.09 ± 0.40	1.96 ± 0.30	1.89 ± 0.29	<0.001
Maximum, mm	3.38 ± 1.16	3.60 ± 1.72	3.24 ± 0.74	3.19 ± 0.72	0.037
Minimum, mm	1.19 ± 0.25	1.27 ± 0.21	1.20 ± 0.24	1.11 ± 0.25	<0.001
ILT thickness					
Mean, mm	4.06 ± 2.08	4.50 ± 2.05	4.05 ± 2.15	3.61 ± 1.97	0.011
Maximum, mm	14.76 ± 6.91	15.73 ± 5.48	14.65 ± 7.17	13.90 ± 7.82	0.173
Minimum, mm	0.90 ± 0.11	0.93 ± 0.15	0.89 ± 0.08	0.89 ± 0.09	0.020
Wall strength					
Mean, MPa	0.76 ± 0.13	0.80 ± 0.09	0.76 ± 0.13	0.71 ± 0.16	<0.001
Maximum, MPa	1.04 ± 0.11	1.08 ± 0.06	1.05 ± 0.09	0.98 ± 0.13	<0.001
Minimum, MPa	0.56 ± 0.12	0.62 ± 0.07	0.57 ± 0.10	0.50 ± 0.15	<0.001

Table 3: Clinical outcomes of patients stratified into peak aneurysm biomechanical ratio (ABR) tertiles. Data are sample size (%) or mean ± standard deviation and p-values are from ANOVA for continuous variables and Chi-squared for categorical variables.

	Tertile 1	Tertile 2	Tertile 3	
Clinical event	**Low ABR**	**Medium ABR**	**High ABR**	**p-value**
Mean follow-up, y	2.98 ± 0.51	3.04 ± 0.48	2.91 ± 0.58	0.346
Repair or rupture	30* (25.4)	36 (31.6)	49 (43.0)	0.010
Repair	24 (24.2)	34 (34.7)	44 (44.9)	0.001
Rupture	6* (6.1)	2 (2.0)	5 (5.1)	0.358

*One ruptured case was repaired and the patient survived.

Table 4: Cox regression analysis for each of the three models and the primary endpoint of repair and/or rupture.

	Hazard ratio (95% CI)	p-value
Model 1		
Aneurysm biomechanical ratio, tertiles	1.42 (1.13-1.79)	0.003
Model 2		
Aneurysm biomechanical ratio, tertiles	1.37 (1.07-1.75)	0.014
Age, y	0.94 (0.91-0.97)	<0.001
Gender	1.01 (0.57-1.78)	0.977
Baseline diameter, mm	1.08 (1.06-1.10)	<0.001
Model 3		
Aneurysm biomechanical ratio, tertiles	1.41 (1.09-1.83)	0.010
Age, y	0.95 (0.92-0.98)	0.001
Gender	0.90 (0.50-1.62)	0.717
Baseline diameter, mm	1.08 (1.06-1.11)	<0.001
Smoker (current), yes/no	1.10 (0.57-2.14)	0.781
Smoker (previous), yes/no	0.75 (0.42-1.35)	0.341
Diabetes Mellitus, yes/no	0.98 (0.53-1.84)	0.960
Systolic blood pressure, mmHg	0.99 (0.97-1.00)	0.025
Diastolic blood pressure, mmHg	1.03 (1.01-1.06)	0.005
USPIO uptake, yes/no	1.23 (0.82-1.84)	0.315

FIGURES

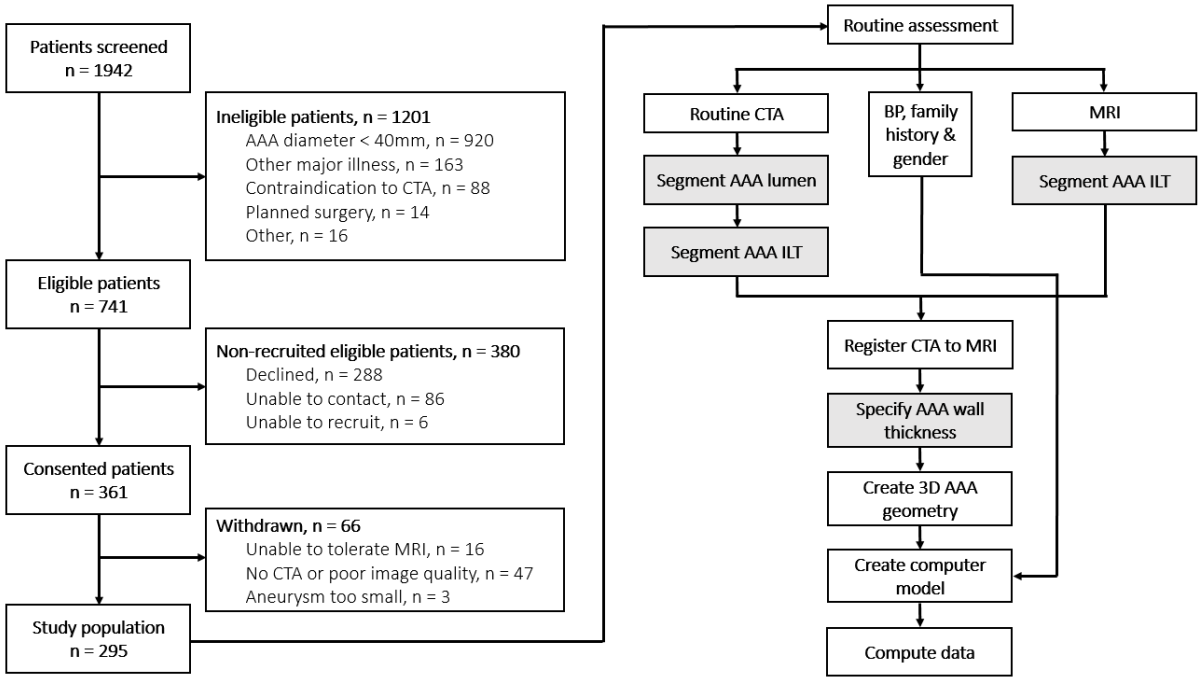

Figure 1: Diagram of participant recruitment (left) and computational workflow of the study (right). The shaded boxes on the right represent steps that require user-input to the computational framework. The computer model uses the finite element method to calculate wall stress with patient-specific systolic blood pressure as input, wall thickness measurements from merged MRI and CTA, and a computational method independent of material properties.[11] CTA = computed tomography angiography; MRI = magnetic resonance imaging; BP = blood pressure; ILT = intraluminal thrombus.

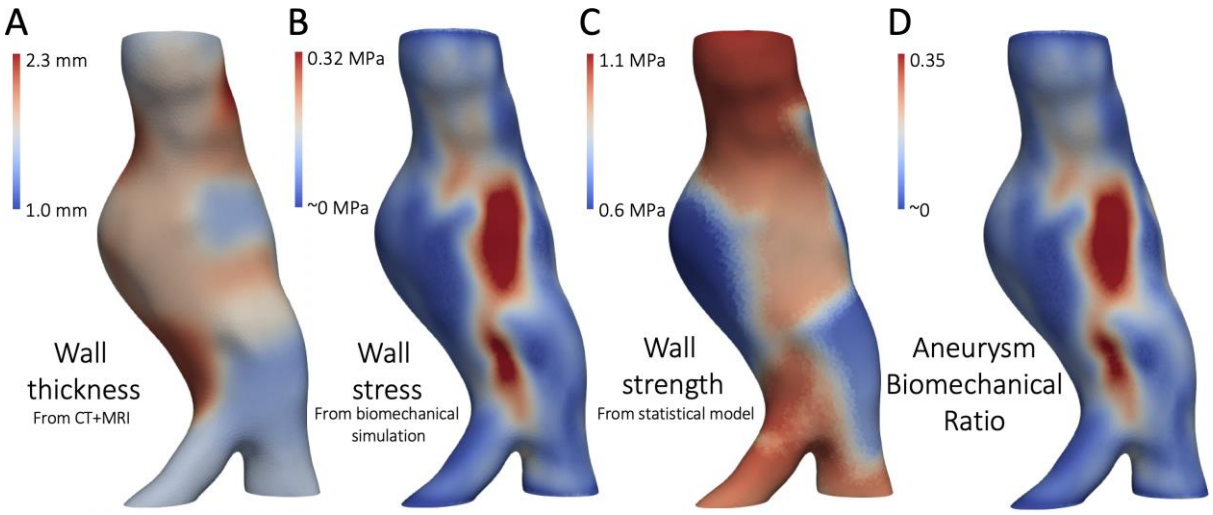

Figure 2: Example biomechanical data produced in the study. (A) Wall thickness is measured on registered MRI-CTA and incorporated into the 3D geometry for more accurate biomechanical simulations. (B) Maximum principal wall stress (units are Megapascal, MPa) is calculated using patient-specific blood pressure measured at the time of baseline imaging. (C) Wall strength is calculated using a previous method[27] that includes factors shown to influence wall strength; patient gender, family history of AAA, local measures of ILT thickness and ratios of local AAA diameter to proximal non-aneurysmal diameter. (D) Aneurysm biomechanical ratio (ABR) is the dimensionless ratio of local wall stress and wall strength and is computed pointwise on the geometry. All data are automatically reported for further analyses.

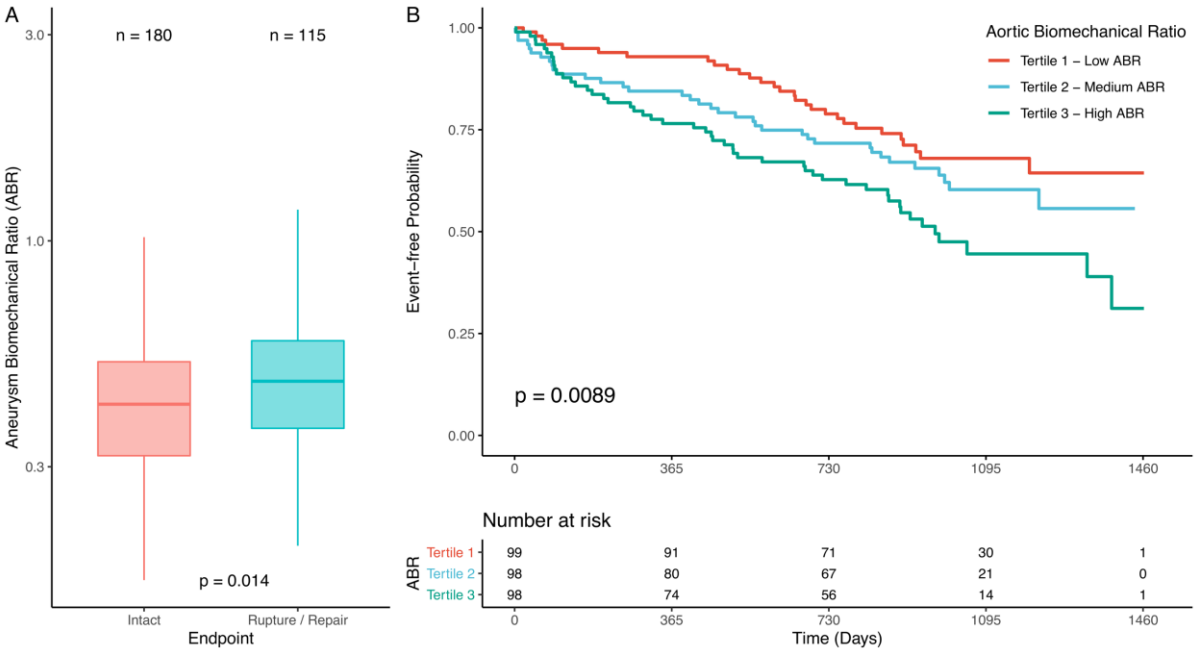

Figure 3: (A) Log-transformed aneurysm biomechanical ratio (ABR) and the primary endpoint. ABR was higher in cases that needed AAA repair or experienced rupture (mean ± standard error Intact vs Ruptured/Repaired; -0.86 ± 0.03 vs. -0.74 ± 0.04; p=0.0138). (B) Kaplan Meier analysis showing time to endpoint. Cases with high ABR at baseline (tertile 3) have significantly poorer outcomes (log rank p-value = 0.0089).

SUPPLEMENTARY MATERIAL

Biomechanical assessment at baseline predicts aneurysm-related events in patients with abdominal aortic aneurysm

Barry J. Doyle,[a,b,c,d] Nikhilesh Bappoo,[a,b] Maaz Syed,[c] Rachael O. Forsythe,[c] Janet T. Powell,[e] Noel Conlisk,[c] Peter R. Hoskins,[c] Grand Roman Joldes,[b] Olivia M.B. McBride,[c] Anoop S.V. Shah,[c] Paul E. Norman,[a,f] David E. Newby[c]

g. Vascular Engineering Laboratory, Harry Perkins Institute of Medical Research, QEII Medical Centre, Nedlands and Centre for Medical Research, The University of Western Australia, Perth, Australia.
h. School of Engineering, The University of Western Australia, Perth, Australia.
i. BHF Centre for Cardiovascular Science, The University of Edinburgh, Edinburgh, UK.
j. Australian Research Council Centre for Personalised Therapeutics Technologies, Australia
k. Vascular Surgery Research Group, Imperial College London, London, UK.
l. Medical School, The University of Western Australia, Perth, Australia.

Address for Correspondence:
Name: Barry Doyle
Address: Harry Perkins Institute of Medical Research, 6 Verdun Street, Nedlands, Western Australia, 6009, Australia.
Tel: +61 8 6151 1084
Fax: +61 8 6151 1084
Email: barry.doyle@uwa.edu.au
Twitter: @vasclab_uwa

Additional Methods
STROBE Checklist

Table S1: Checklist of items. MS Page = manuscript page number; SM Page = Supplementary Material page number (note that page numbers are inconsistent in this version of paper).

	Item No	Recommendation	MS Page	SM Page
Title and abstract	1	(*a*) Indicate the study's design with a commonly used term in the title or the abstract	1	
		(*b*) Provide in the abstract an informative and balanced summary of what was done and what was found	2	
Introduction				
Background/rationale	2	Explain the scientific background and rationale for the investigation being reported	4	
Objectives	3	State specific objectives, including any prespecified hypotheses	5	
Methods				
Study design	4	Present key elements of study design early in the paper	6	
Setting	5	Describe the setting, locations, and relevant dates, including periods of recruitment, exposure, follow-up, and data collection	6	30
Participants	6	(*a*) Give the eligibility criteria, and the sources and methods of selection of participants. Describe methods of follow-up	6	30
		(*b*) For matched studies, give matching criteria and number of exposed and unexposed	NA	
Variables	7	Clearly define all outcomes, exposures, predictors, potential confounders, and effect modifiers. Give diagnostic criteria, if applicable	7,8	
Data sources/ measurement	8*	For each variable of interest, give sources of data and details of methods of assessment (measurement). Describe comparability of assessment methods if there is more than one group	7,8	
Bias	9	Describe any efforts to address potential sources of bias	7	44
Study size	10	Explain how the study size was arrived at	7	
Quantitative variables	11	Explain how quantitative variables were handled in the analyses. If applicable, describe which groupings were chosen and why	8	
Statistical methods	12	(*a*) Describe all statistical methods, including those used to control for confounding	7,8	
		(*b*) Describe any methods used to examine subgroups and interactions	8	
		(*c*) Explain how missing data were addressed	10, Table 1	
		(*d*) If applicable, explain how loss to follow-up was addressed		33
		(*e*) Describe any sensitivity analyses		44
Results				
Participants	13*	(a) Report numbers of individuals at each stage of study—eg numbers potentially eligible, examined for eligibility, confirmed eligible, included in the study, completing follow-up, and analysed	9	
		(b) Give reasons for non-participation at each stage	NA	
		(c) Consider use of a flow diagram	Figure 1	
Descriptive data	14*	(a) Give characteristics of study participants (eg demographic, clinical, social) and information on exposures and potential confounders	Table 1	
		(b) Indicate number of participants with missing data for each variable of interest	10	33
		(c) Summarise follow-up time (eg, average and total amount)	10	
Outcome data	15*	Report numbers of outcome events or summary measures over time	10	

Main results	16	(*a*) Give unadjusted estimates and, if applicable, confounder-adjusted estimates and their precision (eg, 95% confidence interval). Make clear which confounders were adjusted for and why they were included	11-13	39-43
		(*b*) Report category boundaries when continuous variables were categorized	9, Table 1	
		(*c*) If relevant, consider translating estimates of relative risk into absolute risk for a meaningful time period	NA	
Other analyses	17	Report other analyses done—eg analyses of subgroups and interactions, and sensitivity analyses		36-48
Discussion				
Key results	18	Summarise key results with reference to study objectives	12	
Limitations	19	Discuss limitations of the study, taking into account sources of potential bias or imprecision. Discuss both direction and magnitude of any potential bias	14	
Interpretation	20	Give a cautious overall interpretation of results considering objectives, limitations, multiplicity of analyses, results from similar studies, and other relevant evidence	WTPA	
Generalisability	21	Discuss the generalisability (external validity) of the study results	14	
Other information				
Funding	22	Give the source of funding and the role of the funders for the present study and, if applicable, for the original study on which the present article is based	15	

Study design, setting and population

This was a multicentre cohort study performed as part of the MA^{3}RS Study (ISRCTN76413758). Patients were identified from the clinical aneurysm surveillance database at the Royal Infirmary Edinburgh, Western Infirmary Glasgow and Forth Valley Royal Hospital and supplied with information about the study. From the original screening (Figure 1), patients were selected based on inclusion criteria of age ≥ 40 years, aneurysm diameter ≥ 40 mm measured by ultrasound (inner-to-inner AAA wall, anterior-posterior), and under ultrasound surveillance as part of routine care. Patients were excluded if surgical repair was already planned, they had an inflammatory and/or saccular aneurysm, connective tissue disorder, women of childbearing potential, renal failure, contraindication to magnetic resonance imaging (MRI) or ferumoxytol (a contrast agent of ultrasmall superparamagnetic particles of iron oxide (USPIO) required for additional imaging studies), or inadequate image quality for analysis.

From 1942 patients, 1201 were ineligible due to AAA diameter < 40 mm (n=920), other major illness (n=163), contraindication to scan (n=88), planned surgery (n=14), other (n=16). Of the 741 eligible patients, 288 declined, 86 were uncontactable and 6 could not be recruited. Of the resulting 361 patients, 16 were unable to tolerate MRI at time of imaging and 3 had an aneurysm that was too small when imaged with CTA. This left 342 patients who gave informed consent. Cases were then further excluded if the CTA data were missing, incomplete or of poor quality (e.g. imaging artefacts) (n=47). Our cohort had similar characteristics to the original cohort (Table S2).

Table S2: Comparison of this current cohort with the original MA^{3}RS cohort.

	Current cohort (n=295)	**MA3RS Cohort** (n=342)
Characteristics		
Male, %	87.1	85.4
Age, yrs (SD)	73.7 (7.2)	73.1 (7.2)
Smoking status		
Current, %	28.8	29.5
Previous, %	58.0	57.0
Never, %	13.2	13.5
Systolic blood pressure, mmHg	139.8 (24.6)	139.6 (21.2)
Diastolic blood pressure, mmHg	81.4 (11.7)	81.4 (10.8)
Heart rate, bpm*	70.5 (11.4)	70.7 (10.1)
Hypertension, %	72.2	71.9
Aneurysm		
AAA diameter, mm (SD)	49.0 (6.9)	49.6 (7.7)
Rupture/repair, %	38.9	40.9
Rupture, %	4.4	5.0
Rupture, %	34.6	36.8
Medical history		
Diabetes, %	14.2	13.7
Hypercholesterolemia, %	76.6	75.1
Ischaemic heart disease, %	38.0	36.5
Peripheral vascular disease, %	19.7	19.3
Cerebrovascular disease, %	13.2	13.5
Family history of AAA, %	17.6	17.8

Study protocol and follow-up

Within six weeks of the initial screening ultrasound, participants underwent full clinical assessment, including blood pressure measurement, MRI and computed tomography angiography (CTA). MRI protocols have been reported elsewhere and CTA was per routine practice. Patients were then reviewed every six months for a minimum of 24 months, which consisted of maximum anterior-posterior diameter measured by ultrasound at dedicated screening clinics, as well as structured collection of follow-up data and clinical events. The entire protocol describing the study design, collection of clinical data (imaging protocols and data analyses), criteria for surgery and clinical follow-up have been reported previously.

Biomechanical analyses at baseline

Briefly, our process begins by spatially registering the MRI and CTA together into a single image dataset. Aortic wall thickness is measured throughout the aneurysm on the merged images. The aneurysm, including the intraluminal thrombus (ILT), is semi-automatically segmented and reconstructed into three dimensions (3D) using well-established algorithms, after which the non-uniform AAA wall is generated according to the wall thickness data.

After 3D reconstruction, the computational biomechanics processes are fully automated. This process involves creating a volume mesh of finite elements and assigning material properties; these arbitrary properties have no effect on the simulation and are simply required to aid the computation (see Table S5, for further details on the influence of material properties). Patient-specific baseline blood pressure is applied to the inner surface of the lumen and the AAA geometry is fixed from movement in all directions in the proximal and distal regions to represent attachment to the proximal non-aneurysmal aorta and distally to the iliac arteries (Figure S1).

In addition, we investigated the spatial locations of peak ABR in each case by dividing the AAA into regions of interest: posterior, anterior, left and right lateral, and also proximal, medial and distal regions (Figure S3).

Boundary Conditions for Computational Model

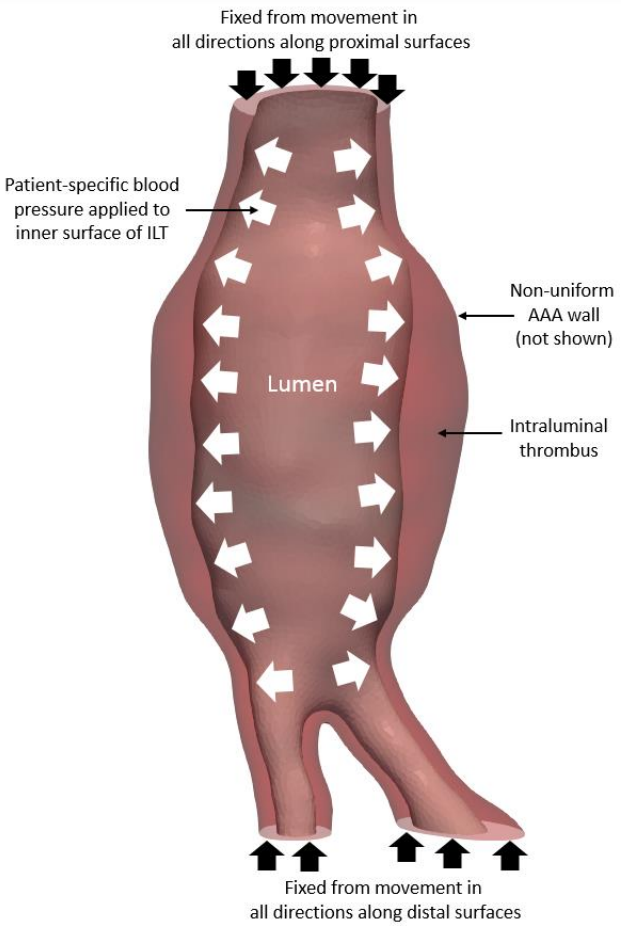

Figure S1: Illustration of boundary conditions used. The AAA geometry was fixed from all movement in the proximal and distal regions to represent attachment to the proximal non-aneurysmal aorta and attachment distally to the iliac arteries. Patient-specific blood pressure was applied to the inner surface of the intraluminal thrombus. This is a widely implemented computational approach in biomechanical analyses.

Missing Growth Rate Data

Growth rate was not available in 46 cases, either due to repair prior to follow-up ultrasound (n=37) or death (AAA rupture, n=2; myocardial infarction, n=1; cancer, n=1; other cause, n=1).

A further three cases of large AAA in elderly men were not repaired as they were unfit for surgery or declined. One case with a small AAA (36 mm) was lost to follow-up after initial US.

Correlations Between Aneurysm Biomechanical Ratio, Peak Wall Stress and Factors That Influence Biomechanical Data

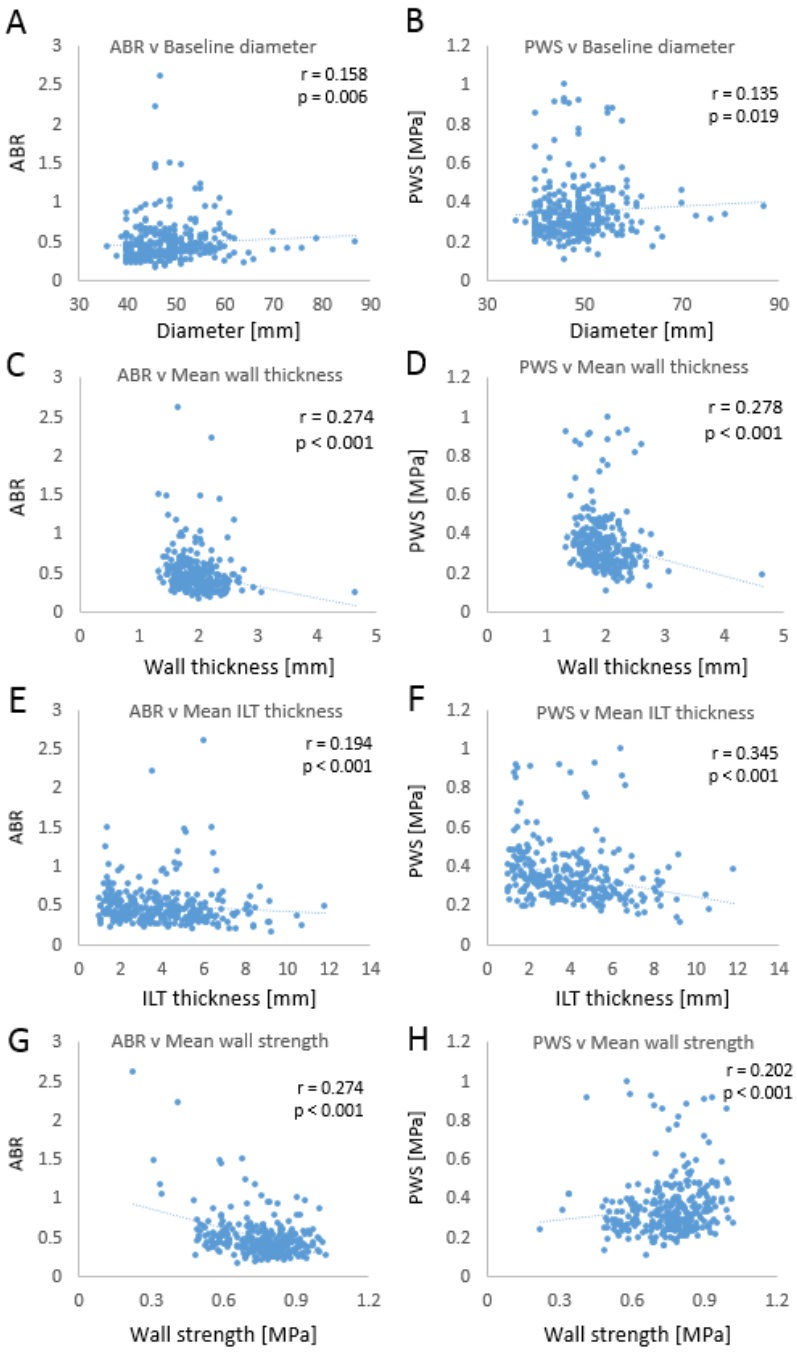

Figure S2: Left column; correlations between aneurysm biomechanical ration (ABR) and (a) baseline diameter, (c) mean wall thickness, (e) mean ILT thickness and (g) mean wall strength. Right column; correlations between peak wall stress (PWS) and (b) baseline diameter, (d) mean wall thickness, (f) mean ILT thickness and (h) mean wall strength.

Location of Peak Aneurysm Biomechanical Ratio

We classified the location of peak aneurysm biomechanical ratio (ABR) for each case according to Figure S3 and the resulting locations are shown in Tables S3-4, and Figure S4.

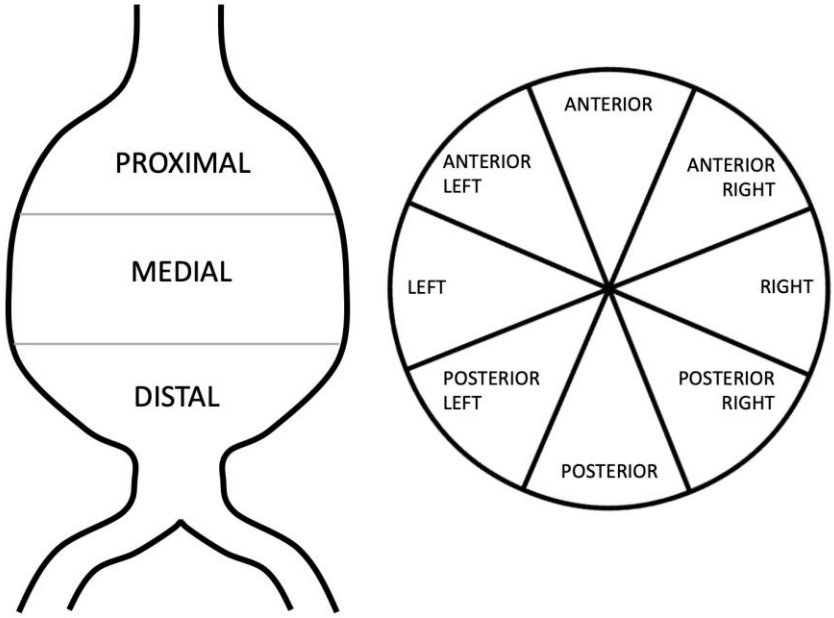

Figure S3: Regions used to mark the location of peak ABR on each AAA. We divided the AAA into proximal, medial and distal with each region accounting for one third of the aneurysm surface area, as shown on the left. We also divided the cross-section as shown on the right. This resulted in 24 anatomical regions.

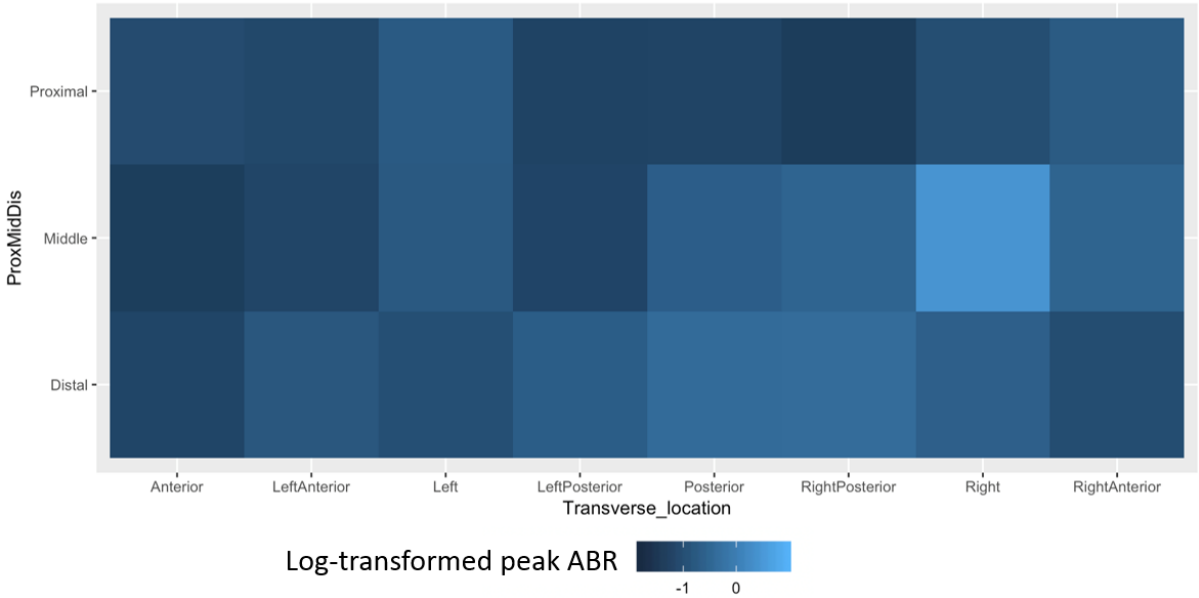

Figure S4: Heat map of log-transformed ABR for each region of interest. The magnitude of ABR was greatest in the right medial region.

Table S3: Locations of peak ABR in the entire cohort as well as for those with and without a clinical event. Data shown as n (%).

Location of peak ABR	All cases	Intact	Repaired	Ruptured
Left Medial	44 (14.9)	25 (13.9)	15 (13.2)	4 (30.8)
Posterior Medial	25 (8.5)	16 (8.9)	6 (5.3)	3 (23.1)
Anterior Medial	19 (6.4)	12 (6.7)	7 (6.1)	-
Posterior Left Medial	19 (6.4)	12 (6.7)	6 (5.3)	1 (7.7)
Anterior Left Medial	17 (5.8)	10 (5.6)	7 (6.1)	-
Posterior Left Distal	16 (5.4)	9 (5%)	7 (6.1)	-
Posterior Right Proximal	16 (5.4)	9 (5%)	7 (6.1)	-
Posterior Proximal	15 (5.1)	9 (5%)	5 (4.4)	1 (7.7)
Left Proximal	14 (4.7)	8 (4.4)	5 (4.4)	1 (7.7)
Left Distal	13 (4.4)	8 (4.4)	5 (4.4)	-
Anterior Proximal	11 (3.7)	6 (3.3)	5 (4.4)	-
Anterior Left Proximal	10 (3.4)	6 (3.3)	4 (3.5)	-
Posterior Right Distal	10 (3.4)	6 (3.3)	3 (2.6)	1 (7.7)
Right Medial	9 (3.1)	6 (3.3)	3 (2.6)	-
Posterior Left Proximal	9 (3.1)	6 (3.3)	3 (2.6)	-
Anterior Right Proximal	8 (2.7)	6 (3.3)	2 (1.8)	-
Posterior Distal	8 (2.7)	6 (3.3)	2 (1.8)	-
Anterior Right Medial	7 (2.4)	5 (2.8)	2 (1.8)	-
Anterior Distal	5 (1.7)	3 (1.7)	2 (1.8)	-
Anterior Right Distal	5 (1.7)	3 (1.7)	1 (0.9)	1 (7.7)
Right Proximal	5 (1.7)	3 (1.7)	2 (1.8)	-
Right Distal	4 (1.4)	3 (1.7)	1 (0.9)	-
Anterior Left Distal	3 (1.0)	2 (1.1)	1 (0.9)	-
Posterior Right Medial	3 (1.0)	2 (1.1)	-	1 (7.7)

Table S4: Locations of peak ABR across the tertiles of peak ABR. Data shown as n (%).

	Tertile 1	Tertile 2	Tertile 3
Location of peak ABR	**Low ABR**	**Medium ABR**	**High ABR**
Left Medial	11 (11.1)	15 (15.3)	18 (18.4)
Posterior Medial	8 (8.1)	6 (5.3)	8 (8.2)
Anterior Medial	5 (5.1)	6 (6.1)	8 (8.2)
Posterior Left Medial	5 (5.1)	6 (6.1)	8 (8.2)
Anterior Left Medial	8 (8.1)	5 (5.1)	4 (4.1)
Posterior Left Distal	5 (5.1)	6 (6.1)	5 (5.1)
Posterior Right Proximal	5 (5.1)	7 (7.1)	4 (4.1)
Posterior Proximal	8 (8.1)	3 (3.1)	4 (4.1)
Left Proximal	7 (7.1)	3 (3.1)	4 (4.1)
Left Distal	5 (5.1)	5 (5.1)	3 (3.1)
Anterior Proximal	5 (5.1)	3 (3.1)	3 (3.1)
Anterior Left Proximal	3 (3.0)	4 (4.1)	3 (3.1)
Posterior Right Distal	3 (3.0)	2 (2.0)	5 (5.1)
Right Medial	5 (5.1)	2 (2.0)	2 (2.0)
Posterior Left Proximal	3 (3.0)	4 (4.1)	2 (2.0)
Anterior Right Proximal	2 (2.0)	4 (4.1)	2 (2.0)
Posterior Distal	2 (2.0)	3 (3.1)	3 (3.1)
Anterior Right Medial	-	4 (4.1)	3 (3.1)
Anterior Distal	2 (2.0)	2 (2.0)	1 (1.0)
Anterior Right Distal	2 (2.0)	-	3 (3.1)
Right Proximal	2 (2.0)	2 (2.0)	1 (1.0)
Right Distal	2 (2.0)	-	2 (2.0)
Anterior Left Distal	-	2 (2.0)	1 (1.0)
Posterior Right Medial	1 (1.0)	1 (1.0)	1 (1.0)

Post Hoc Analysis of Growth Rate as the Endpoint

The original composite endpoint was rupture or repair. We also performed a post hoc analysis using a generalised model with growth rate as the endpoint. The same predictors were then used as in the original Cox Survival analysis: Aneurysm Biomechanical Ratio, age, sex, AAA size (at baseline), smoking status, systolic blood pressure, diastolic blood pressure, diabetes mellitus and USPIO uptake, resulting in three models as before. Each regression model then created a binary endpoint depending on the growth rate threshold applied. Here we chose 2.5 mm/y which is the slightly greater than the mean growth rate of small AAAs[1] and slightly below the mean growth rate determined in our cohort (2.84 mm/y). We then run each model ten times with an incremental increase in AAA growth rate by 0.5 mm/yr. Guidelines recommend intervening when growth rate exceeds 10 mm/y, however very few cases which such growth exist in our cohort (n=3), so we have limited our analysis to annual growth of 5 mm/y.

Using a 2.5 mm/y threshold for growth rate, we find the following odds ratios.

- *Model 1:* OR 1.51 (1.29-1.77); p<0.001
- *Model 2:* OR 1.58 (0.73-3.41); p=0.248
- *Model 3:* OR 1.32 (0.49-3.53); p=0.586

The full analyses for each model are presented in Figures S5-7. In essence, ABR predicts growth up to 1.5 mm/y but not beyond this when adjusted for other risk factors.

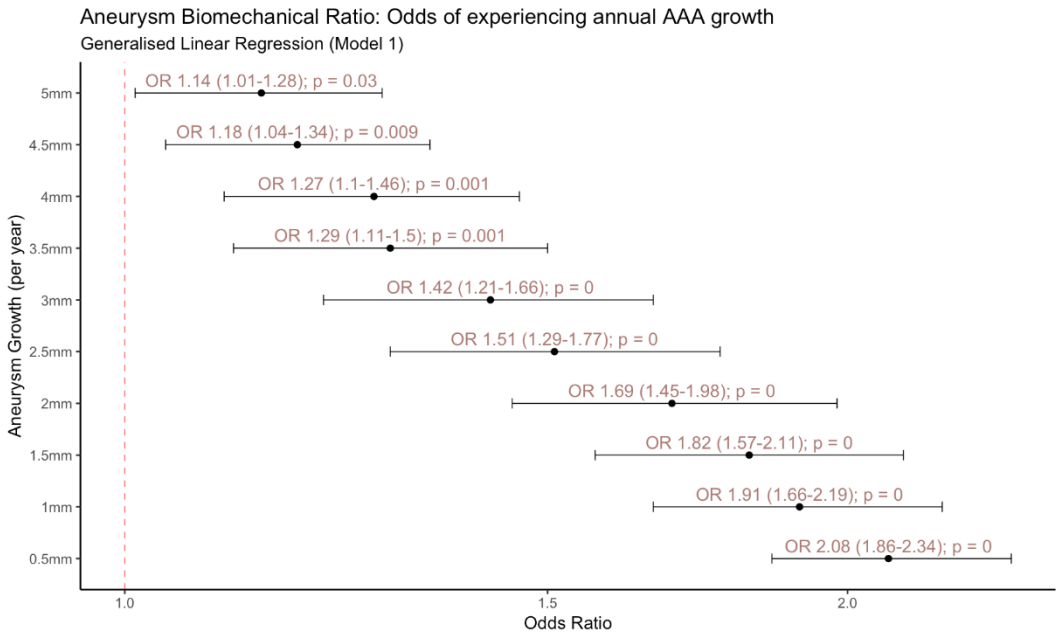

Figure S5: Aneurysm biomechanical ratio as a sole predictor of experiencing annual aortic growth (generalised linear regression model – Model 1).

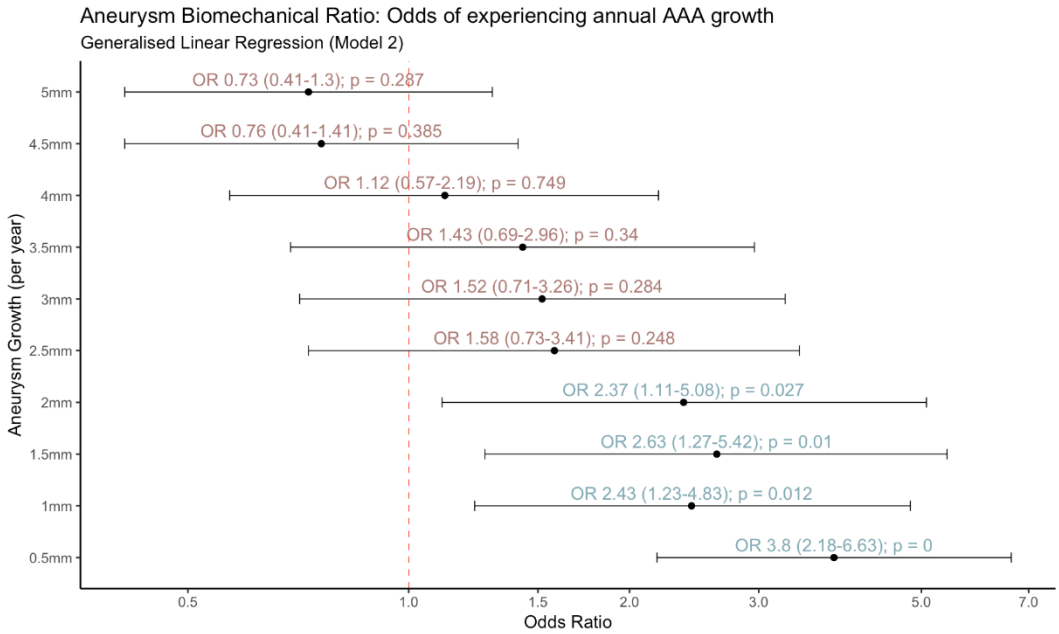

Figure S6: Aneurysm biomechanical ratio as a predictor of experiencing annual aortic growth following adjustment for age, gender and baseline AAA diameter from ultrasound (generalised linear regression – Model 2).

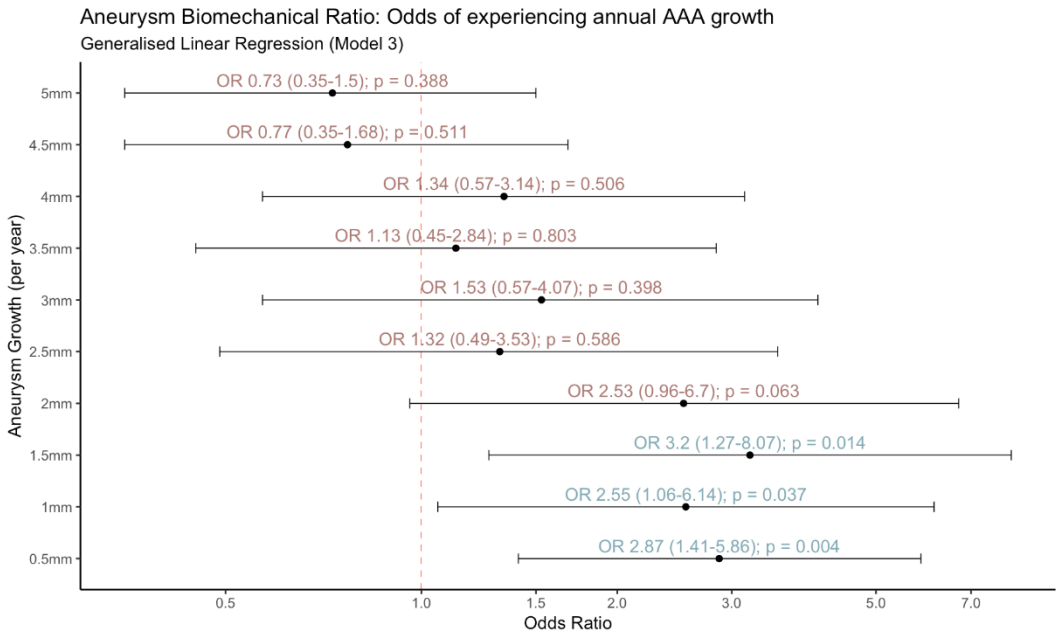

Figure S7: Aneurysm biomechanical ratio as a predictor of experiencing annual aortic growth following adjustment for age, gender, baseline AAA size from ultrasound, smoking status, blood pressure, diabetes mellitus and USPIO uptake (generalised linear regression – Model 3).

Categorical Net Reclassification Index at 0.5 Risk Threshold

Figure S8: Net reclassification index of our new model at a risk threshold of 0.5, split into peak ABR tertiles. The NRIcat value was 0.066 (95% CI, -0.011-0.142; p=0.093) with 16 cases reclassified up and 7 reclassified down.

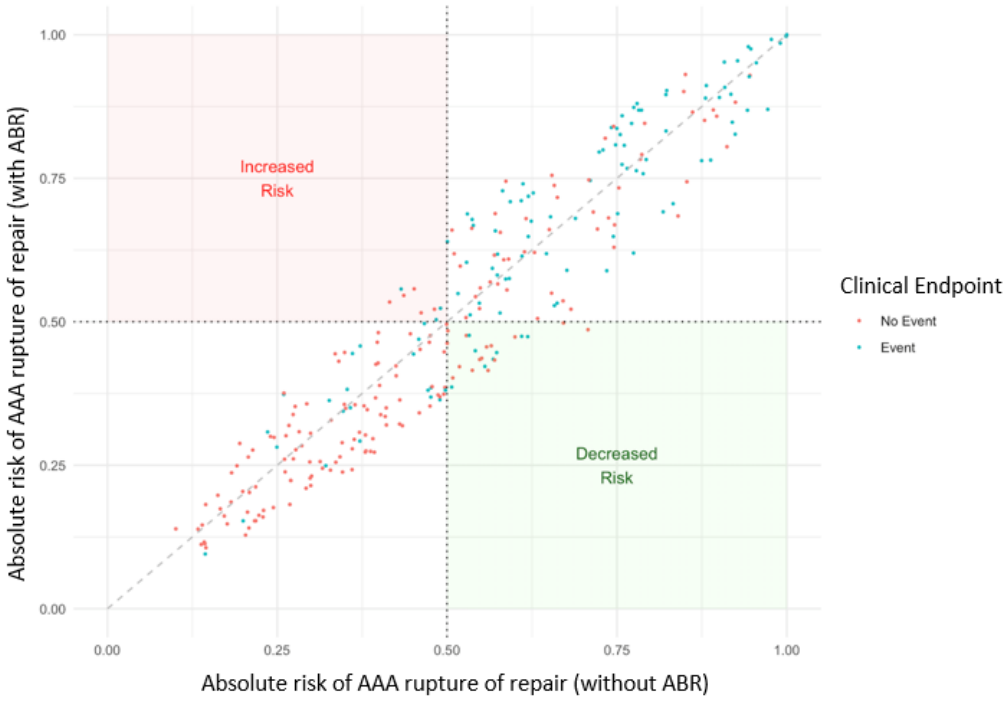

Figure S9: Net reclassification index of our new model at a risk threshold of 0.5, split into those who did and did not have a clinical event.

Categorical Net Reclassification Index at 0.8 Risk Threshold

Figure S10: Net reclassification index of our new model at a risk threshold of 0.8, split into peak ABR tertiles. NRIcat value was 0.011 (95% CI, -0.064-0.086; p=0.769) with 8 cases reclassified up to a higher risk and 23 reclassified down to a lower risk.

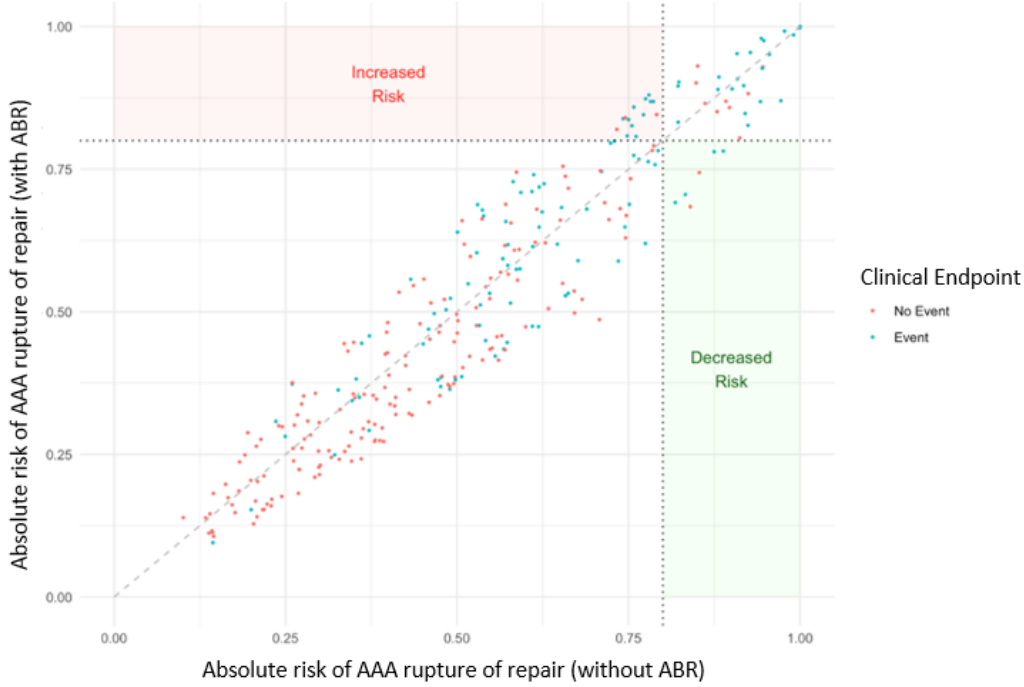

Figure S11: Net reclassification index of our new model at a risk threshold of 0.8, split into those who did and did not have a clinical event.

The Influence of Computational Methods

We also wanted to explore and understand the influence of modelling approach on the biomechanical data of our cohort. *In vivo* patient-specific material properties are unknown and introduce major uncertainty[2] without modelling the AAA as statically determinate[3-5] or using inverse modelling methods.[6] Therefore, in order for biomechanical methods to be used with confidence in the clinic, the only practical approach is to remove material properties from the solution completely, similar to our approach in this study.

In order to demonstrate the effect of common modelling assumptions in AAA biomechanical analyses, we studied a sub-group from our cohort (n=15) using commercial methods (A4research™, VASCOPS GmbH, Graz, Austria) that have been widely adopted (e.g. Leemans et al.[7]). By implementing the statically determinate approach, we tested the effect of patient-specific wall thickness compared to the variable wall model implemented in A4research™. We found that maximum principal wall stresses (i.e. PWS) were on average 24% higher (range 4-48%, p=0.0002; Table S5) when including patient-specific wall thickness.

We also compared PWS computed using the common assumption of uniform wall thickness (1.5 mm) compared to the patient-specific geometry with measured wall thickness, again using the statically determinate approach. Wall stress varied by an average of 11% (range 0-39%, p=0.3462; Table S6), with similarly large percentage differences also reported previously.[8]

Finally, we tested the effect of simulation strategy by comparing the statically determinate linear simulations to the commonly used non-linear method (also implemented in

A4research™). We found PWS to differ on average by 18% (range 1-34%, p=0.0140; Table S7) with 10/15 cases experiencing ≥ 10% difference.

Therefore, our data indicate that even with a thorough understanding of the level of uncertainty in computational simulations,[9] it may not be appropriate to use ambiguous biomechanical models to assess potentially life-threatening aneurysms. Unknown material properties and wall thickness represent major obstacles to current biomechanical methods, hence why we have developed our approach. Importantly, others are also developing methods of calculating aortic wall stress without material properties[5, 10] or with estimates of wall thickness[11,12] as sensible ways to implement computational biomechanics simulations in the clinic.

Table S5: Effect of reconstruction process on the maximum principal wall stress. Data shows the wall stress computed using the variable wall thickness algorithm of A4research™ and the patient-specific measurements used here. We used the same material properties, pressure loading and constraints for both simulations. We calculated the percentage change relative to our data. The difference in wall stress was significant (p=0.0002) using a two-sided Mann-Whitney test.

	Max principal stress (MPa)		
Case	**A4research™**	**Our approach**	**% change**
1	0.223	0.243	8.1
2	0.232	0.287	19.2
3	0.292	0.412	29.1
4	0.227	0.438	48.1
5	0.210	0.312	32.7
6	0.200	0.242	17.5
7	0.213	0.254	16.1
8	0.227	0.218	3.9
9	0.171	0.228	25.3
10	0.176	0.229	23.3
11	0.152	0.231	34.1
12	0.183	0.245	25.1
13	0.217	0.242	10.4
14	0.210	0.286	26.8
15	0.151	0.235	35.9
Mean	0.206	0.276	23.7
SD	0.036	0.057	11.7
Min	0.151	0.228	3.9
Max	0.292	0.438	48.1

Table S6: Effect of wall thickness on the maximum principal wall stress. Data shows the wall stress computed using a typically employed uniformly thick AAA wall (1.5 mm) and that of the patient-specific measurements used here. We used the same material properties, pressure loading and constraints for both simulations. We calculated the percentage change relative to the patient-specific data. The difference in wall stress was not significant (p=0.3462) using a two-sided Mann-Whitney test.

	Max principal stress (MPa)		
Case	**Constant**	**Patient-specific**	**% change**
1	0.250	0.243	3.1
2	0.303	0.287	5.7
3	0.496	0.412	20.3
4	0.402	0.438	8.1
5	0.324	0.312	4.0
6	0.337	0.242	39.3
7	0.237	0.254	6.6
8	0.253	0.218	15.7
9	0.215	0.228	5.9
10	0.264	0.229	15.1
11	0.200	0.231	13.5
12	0.277	0.245	13.2
13	0.254	0.242	4.7
14	0.286	0.286	0.2
15	0.254	0.235	8.1
Mean	0.281	0.276	10.9
SD	0.058	0.057	9.6
Min	0.200	0.228	0.2
Max	0.405	0.438	39.3

Table S7: Effect of simulation strategy on the maximum principal wall stress. Data shows the wall stress computed using the non-linear material properties implemented in A4research™, compared to the statically determinate linear method we use. We used the same geometries (both created with A4research™), pressure loading and constraints for both simulations. We calculated the percentage change relative to our linear data. The difference in mean wall stress was significant (p=0.0140) using a two-sided Mann-Whitney test.

	Max principal stress (MPa)		
Case	**Non-linear**	**Linear**	**% change**
1	0.220	0.223	1.4
2	0.220	0.232	5.1
3	0.196	0.292	32.8
4	0.186	0.227	18.2
5	0.141	0.210	33.1
6	0.191	0.200	4.5
7	0.191	0.213	10.3
8	0.163	0.227	28.2
9	0.118	0.171	30.9
10	0.158	0.176	10.3
11	0.142	0.152	6.5
12	0.185	0.183	0.8
13	0.144	0.217	33.5
14	0.140	0.210	33.1
15	0.188	0.151	24.8
Mean	0.172	0.206	18.2
SD	0.031	0.036	13.1
Min	0.118	0.151	0.8
Max	0.220	0.292	33.5

REFERENCES

1. Sweeting MJ, Thompson SG, Brown LC, Powell JT on behalf of the RESCAN Collaborators. Meta-analysis of individual patient data to examine factors affecting growth and rutpure of small abdominal aortic aneurysms. Br J Surg. 2012;99:655-65.
2. Doyle BJ, Callanan A, Grace PA and Kavanagh EG. On the influence of patient-specific material properties in computational simulations: A case study of a large ruptured abdominal aortic aneurysm. *Int J Numer Meth Biomed Engng*. 2013;29:150-164.
3. Joldes GR, Miller K, Wittek A and Doyle B. A simple, effective and clinically applicable method to compute abdominal aortic aneurysm wall stress. *J Mech Behav Biomed Mater*. 2016;58:139-48.
4. Joldes GR, Miller K, Wittek A, Forsythe RO, Newby DE and Doyle BJ. BioPARR: A software system for estimating the aneurysm biomechanical ratio for abdominal aortic aneurysms. *Sci Rep*. 2017;7:4641.
5. Liu M, Liang L, Liu H, Zhang M, Martin C and Sun W. On the computation of in vivo transmural mean stress of patient-specific aortic wall. *Biomech Model Mechanobiol*. 2018.
6. Lu J, Zhou X and Raghavan ML. Inverse elastostatic stress analysis in pre-deformed biological structures: Demonstration using abdominal aortic aneurysms. *J Biomech*. 2007;40:693-6.
7. Leemans EL, Willems TP, Slump CH, van der Laan MJ and Zeebregts CJ. Additional value of biomechanical indices based on CTa for rupture risk assessment of abdominal aortic aneurysms. *PLOS ONE*. 2018;13:e0202672.

8. Conlisk N, Geers AJ, McBride OM, Newby DE and Hoskins PR. Patient-specific modelling of abdominal aortic aneurysms: The influence of wall thickness on predicted clinical outcomes. *Med Eng Phys*. 2016;38:526-37.

9. Polzer S and Gasser TC. Biomechanical rupture risk assessment of abdominal aortic aneurysms based on a novel probabilistic rupture risk index. *J Roy Soc Inter*. 2015;12:20150852.

10. Lu J and Luo Y. Solving membrane stress on deformed configuration using inverse elastostatic and forward penalty methods. *Comp Meth Appl Mech Engng*. 2016;308:134-150.

11. Shum J, Di Martino ES, Goldhamme A, Goldman DH, Acker LC, Patel G, Ng JH, Martufi G and Finol EA. Semiautomatic vessel wall detection and quantification of wall thickness in computed tomography images of human abdominal aortic aneurysms. *Med Phys*. 2010;37:638-48.

12. Shang EK, Nathan DP, Woo EY, Fairman RM, Wang GJ, Gorman RC, Gorman JH, 3rd and Jackson BM. Local wall thickness in finite element models improves prediction of abdominal aortic aneurysm growth. *J Vasc Surg*. 2015;61:217-23.